Iron content of functional networks in the aged human cortex

Valerie C. Anderson[1], Manoj K. Sammi[1], Yosef A. Berlow[1], Jeffrey A. Kaye[2], Joseph F. Quinn[2], and William D. Rooney[1]
[1]*Advanced Imaging Research Center, Oregon Health & Science University, Portland, OR, United States,* [2]*Department of Neurology, Oregon Health & Science University, Portland, OR, United States*

Introduction: Brain iron content increases with age[1] and may contribute to the memory decline in older individuals. In the cortex, regional differences in atrophy, thickness, and metabolism have been demonstrated[2] and may account for the variation in cognitive performance frequently observed. The purpose of this study is to characterize the spatial distribution of cortical Fe concentration, [Fe], in the healthy elderly brain and examine the extent to which [Fe] varies in circuits important in cognitive function. To accomplish this, we used a novel quantitative MRI approach combining R_1 and R_2 measurements and relaxivity models that incorporate terms for both the macromolecular volume fraction, f_M, and [Fe].

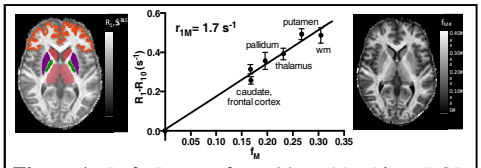

Figure 1. (Left) R_1 map from 66 yr old subject. ROIs were defined in the basal ganglia, frontal cortex and deep white matter (WM; centrum semiovale, not shown). (Middle) Plot of average tissue R_1 vs. post-mortem f_M values[1]. Error bars indicate 1 SD. (Right) f_M map from the same subject.

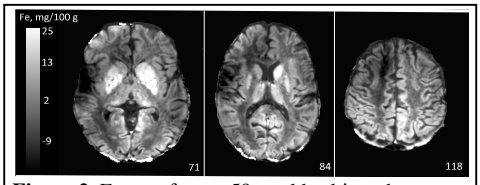

Figure 2. Fe map from a 59 yr old subject shows expected high iron content in basal ganglia. MNI z coordinate of slices shown at lower right.

Methods: 20 healthy older subjects (63 ± 9 yrs; 11 males, 9 females) with no history of neurologic or vascular disease provided informed consent and were enrolled. MR data were acquired on a 7T whole-body instrument (Siemens MAGNETOM) with 8- or 24-channel RF head coil. Anatomic inversion recovery (IR) MPRAGE images (TR/TE/TI/FA 2300 ms/ 2.8 ms/ 1050 ms/ 6°; 0.8 mm^3) were acquired for registration and cortical reconstruction. Full volume R_1 maps were prepared from a variable TI (300, 1800, 3200 ms; and no inversion pulse) IR-MPRAGE (TR/TE/FA 3500 ms/ 2.4 ms/ 6°; nominal in-plane resolution 1 mm^2; 2 mm slice thickness) image set after linear registration (FSL; http://fsl.fmrib.ox.ac.uk) and voxelwise evaluation of the Bloch equations accounting for all RF pulses and delays and assuming monoexponential IR recovery.[3] Bilateral regions of interest (ROI) were defined manually or by segmentation of the co-registered anatomic T_1-weighted image.[4] Macromolec- ular volume fraction ($f_M \equiv$ 1- fractional water content) was determined on a voxelwise basis assuming a linear dependence of tissue R_1 values on f_M.[5] R_2 maps were prepared from a 2D dual echo TSE sequence (TE 11, 87 ms; TR 10000 ms, ETL 7, nominal in-plane resolution 0.44 mm^2, 2 mm slice thickness, 2 mm interslice gap) assuming monoexponential signal intensity decay.

Multivariable linear regression modeling of mean ROI R_2 values using postmortem [Fe][1] and ROI f_M values as independent variables yielded estimates of transverse relaxivity at macromolecular and Fe sites, r_{2M} and r_{2Fe}, respectively. Maps of brain Fe content were calculated assuming $R_2 = R_{20} + r_{2M}f_M + r_{2Fe}$[Fe], where R_{20}= R_2 value of CSF (Eq. 1).[6] Cortical [Fe] was determined after non-linear registration of Fe maps to MNI 152 standard space and preparation of pial surface masks from the anatomic T_1-weighted image (Freesurfer).[7] Application of MNI 152 cortical network masks[8] to Fe pial surface maps yielded estimates of [Fe] in visual (V), somatomotor (S), dorsal attention (DA), ventral attention (VA), frontoparietal (FP), and default (D) networks. All statistical analyses were performed in Stata 12 (College Station, TX). P values were adjusted for multiple comparisons using Tukey HSD.

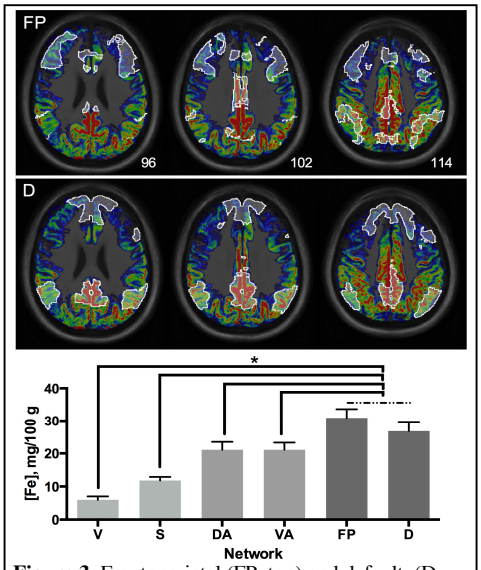

Figure 3. Frontoparietal (FP, top) and default (D, middle) networks (white) superimposed on average [Fe] pial surface map and T_1-w image (MNI z coordinates shown at lower right). Areas of highest [Fe] shown in red. (bottom) Fe content of functional networks. Error bars indicate SEM. * P (corr)< 0.05

Results and Discussion: Linear regression of ROI mean R_1 and f_M values, determined from histogram fittings, yields an r_{1M} value of 1.7 ± 0.3 s^{-1}, in good with that reported previously[5].

Table 1. Mean R_1, R_2 and [Fe] Values in Selected Regions[a]

Region	R_1, s^{-1}	R_2, s^{-1}	R_2, s^{-1} [b]	Fe, mg/100 g	Fe, mg/100 g[c]
Caudate	0.57 ± 0.01	12 ± 1	16.2	10 ± 2	9 ± 2
Pallidum	0.74 ± 0.03	20 ± 2	15 ± 1[d]	20 ± 3	21 ± 3
Putamen	0.61 ± 0.02	16 ± 2	14.2	16 ± 3	13 ± 3
Cortical GM	0.51 ± 0.01	8 ± 1	27.2	5 ± 2	3 ± 0.4
Deep WM	0.74 ± 0.03	11 ± 2	23.6	4 ± 2	4 ± 1

[a] ± SD; [b]Ref. 10; [c]Ref. 1; [d]1.5T, Ref. 11; [e]3T, Ref. 12

Although gray matter (GM) and WM have different chemical composition and morphologies, the linearity of the plot (**Fig. 1**) suggests that r_{1M} does not vary substantially by tissue type at 7T. Multivariable linear modeling of mean ROI R_2 values yields estimates of r_{2Fe} and r_{2M} of 0.58 ± 0.14 s^{-1} per mg Fe/100 g tissue and 18.8 ± 9.8 s^{-1}/f_M, respectively, and confirms that both Fe and macromolecules account for a significant portion of R_2 variability at high field ($F(2, 6) = 155.6$, $P < 0.001$; $P(Fe, f_M) < 0.05$). A representative Fe map is shown in **Fig. 2.** Regional [Fe] estimates calculated from Eq. 1 and summarized in **Table 1** show good agreement with post-mortem values. In cortical networks, mean [Fe] ranged from 5.9- 30.5 mg/100 g ($P < 0.001$). After adjustment for multiple comparisons, Fe content remained significantly higher in both FP and D circuits (**Fig. 3**). Although increased subject numbers will be necessary to confirm these findings, our results suggest that the vulnerability of frontoparietal and default networks to age-related brain changes[9] may be associated with increased iron content.

Grant Support: NIH (AG 033638, AG008017) and NCRR (RR024140-04S1). **Refs**: **1**. Hallgren and Sourander *J Neurochem* 3:41-51 (1958). **2**. van Rooden, et al., *Neurobiol Aging* (2014) doi:10.1016/j.neurobiolaging.2014.07.006. **3.** Deichmann and Haase, *JMR* 96:608-12 (1992). **4**. Smith, et al., *Neuroimage* 17:479-89 (2002). **5**. Rooney, et al., *MRM* 57: 308-18 (2007). **6**. Mitsumori, et al., *MRM* 62:1326-30 (2009). **7**. http://surfer.nmr.mgh.harvard.edu. **8**. Yeo, et al., *J Neurophysiol* 106:1125-65 (2011). **9**. Greenwood, et al., *JINS* 6:705-726 (1999). **10**. Peters, et al., *PISMRM* 14:926 (2006). **11**. Schenker, et al., *Neuroradiology* 35:119-24 (1993). **12**. Hasan, et al., *J Neurosci* 31:16826-32 (2011).